A sensitivity analysis of design parameters of BIPV/T-DSF in relation to building energy and thermal comfort performances

A sensitivity analysis of building-integrated photovoltaic/thermal double-skin façades (BIPV/T-DSF) in various climatic conditions in Australia

Siliang Yang[a,b,*], Francesco Fiorito[a,c], Deo Prasad[a], Alistair Sproul[d]

[a] Faculty of Built Environment, University of New South Wales, Sydney, Australia

[b] School of Built Environment, Engineering and Computing, Leeds Beckett University, Leeds, United Kingdom

[c] Department of Civil, Environmental, Land, Building Engineering and Chemistry, Polytechnic University of Bari, Bari, Italy

[d] School of Photovoltaic and Renewable Energy Engineering, University of New South Wales, Sydney, Australia

* Corresponding author. E-mail address: s.yang@leedsbeckett.ac.uk (Siliang Yang).

ABSTRACT

Building facades play a key role in affecting indoor thermal comfort and energy efficiency of buildings. In recent years, Building-Integrated Photovoltaic/Thermal Double-Skin Façade (BIPV/T-DSF) shows great potentials on improving indoor thermal comfort and reducing energy consumption for the buildings. Previous studies have assessed both indoor thermal comfort and energy performance of the building configured the BIPV/T-DSF. However, the assessments focused merely on the use of the photovoltaic devices and ventilation types of the BIPV/T-DSF and did not involve the effect of other dominant design parameters on the BIPV/T-DSF's performance, which essentially couldn't determine the optimal design solutions. For this reason, this paper presents a simulation study of sensitivity analysis to evaluate how indoor thermal comfort and energy consumption were sensitive to various design parameters of the BIPV/T-DSF operating in different ventilation modes (non-ventilation, natural ventilation and mechanical ventilation) for an office building under a range of climatic conditions across Australia. The study identified the most important design parameters tied to indoor thermal comfort and energy consumption of the building. Results showed that solar heat gain coefficient of the BIPV/T-DSF's external window possessed the highest importance affecting indoor thermal comfort and energy consumption in the either ventilation mode under the either climatic condition. Thermal transmittance of both the internal and external windows and cavity depth of the BIPV/T-DSF showed also the notable importance to the building performances. These most important design parameters are therefore refined to determine the optimal design solution of the BIPV/T-DSF.

Keywords:

Sensitivity analysis; Building-integrated photovoltaic/thermal system; Double-skin façade; Indoor thermal comfort; Energy consumption; TRNSYS simulation

Nomenclature

Symbols

C_L	louvre's opening ratio of double-skin façade [-]
D_{ca}	cavity depth of double-skin facade [m]
E_{max}	maximum output value [-]
E_{min}	minimum output value [-]
Q_{ACH}	air exchange rate of supply fan [ACH]
$q_{comb,s,i}$	combined convective and radiative heat flux in the space [kW]
$q_{comb,s,o}$	combined convective and radiative heat flux to surface [kW]
$q_{s,i}$	conductive heat flux from inside surface [kW]

$q_{s,o}$	conductive heat flux from outside surface [kW]
SHGC	solar heat gain coefficient [-]
$SHGC_{in}$	solar heat gain coefficient of internal window of double-skin façade [-]
$SHGC_{out}$	solar heat gain coefficient of external window of double-skin façade [-]
$S_{s,i}$	solar radiation and long-wave radiation from internal objects [kW]
$S_{s,o}$	solar radiation from external surfaces [kW]
U-value	thermal transmittance [W/m^{2}K]
U_{in}	thermal transmittance of internal window of double-skin façade [W/m^{2}K]
U_{out}	thermal transmittance of external window of double-skin façade [W/m^{2}K]
Wallgain	user-defined energy flow to surfaces of inside wall or window [kW]

Greek symbols

α_P	temperature coefficient of power [%/°C]
η	PV efficiency [%]

Abbreviations

ACH	air changes per hour
BIPV/T-DSF	building-integrated photovoltaic/thermal double-skin facade
COP	coefficient of performance
DSF	double-skin facade
MechVent-DSF	mechanically-ventilated double-skin facade
NatVent-DSF	naturally-ventilated double-skin facade
NoVent-DSF	non-ventilated double-skin facade
PV	photovoltaic
SI	sensitivity index
STC	standard test conditions
VLT	visible light transmittance
WWR	window-to-wall ratio

1. Introduction

Building façade is a major component of the building envelope, which maintains indoor thermal comfort within a building and heavily influences the building energy consumption [1], consequently affects the productivity and environments. Thus, exploring high performance building facades is important to improve indoor thermal comfort as well as energy efficiency of buildings. In this context, a novel façade technology, Building-Integrated Photovoltaic/Thermal Double-Skin Façade (BIPV/T-DSF), came out in recent years, which is designed to contribute to the improvement of indoor thermal comfort and the reduction of energy consumption for buildings.

Specifically, the BIPV/T-DSF possesses the characteristics of the photovoltaic (PV) systems, which converts radiant solar energy into electricity; while the ventilated air cavity of the DSF can reduce the surface temperature of the PV systems when they are integrated in the outer layer of the DSF [2-5]. In addition, a useful thermal energy is gained by collecting hot air through the ventilated air cavity of the BIPV/T-DSF, which can be used to compensate for both the heating and cooling demands of the building [5, 6]. The BIPV/T-DSF also possesses the characteristics of the double-skin facades, which provides protection against the weather and the ventilation in the air cavity is adjustable depending upon the quarter hence delivering a comfortable indoor thermal condition [7, 8].

In previous studies [5, 8-10], we have assessed both the indoor thermal comfort and energy performances of a commercial building configured the BIPV/T-DSF in Australia. However, the performance assessments focused merely on the types of PV panel and ventilation modes of the BIPV/T-DSF. As a matter of fact, other dominant design parameters of the BIPV/T-DSF (for example, the solar heat gain coefficient of the window glazing in the DSF) might also affect the thermal comfort and energy performances of the building in a significant way, and it is crucial to attain the optimal design solution of the BIPV/T-DSF through appropriate selection of design variables [11, 12]. Thus, it is important and worth to investigate the relative importance of all the related design parameters of the BIPV/T-DSF so as to make design process more efficient and structured by focusing on the fewer design parameters, and consequently attains well-directed design solution in controlling energy efficiency and indoor thermal comfort more effectively for buildings.

Sensitivity Analysis is an effective approach to identifying the relative importance of input parameters (the design parameters) to the corresponding output [13]. From the perspective of building design, the Sensitivity Analysis aims to determine the contribution of the individual design variable to total performance of the design solution, and identify the most important design parameters tied to building performance; hence, it focuses the building design and optimisation on the fewer parameters [14]. In regard to building performance simulation, sensitivity analysis is performed by varying input parameters of the building model and computing the changes in model output against the output with initial input parameter values, which is also referred to as a "reference model" [15].

It has been approved that the sensitivity analysis is useful and essential for assessing thermal responses of buildings and the variability of design parameters in building energy simulation [16, 17]. There are no particular rules or procedures conventionalised as the methods of sensitivity analysis as they all come with merits and demerits [18, 19]. However, the most typical steps of sensitivity analysis in the field of building performance analysis are summarised in Figure 1.

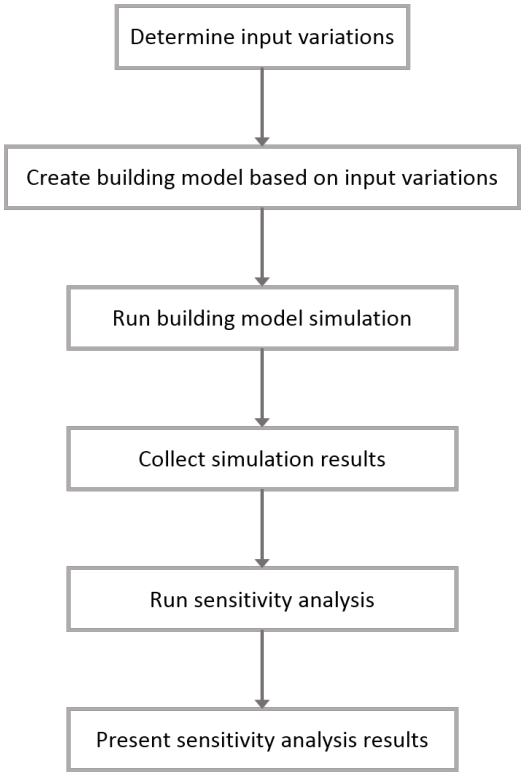

Figure 1. Typical steps of sensitivity analysis for building performance analysis [20].

Basically, the methods of sensitivity analysis in building performance analysis can be broadly categorised into local and global methods [21-24]. Local sensitivity analysis method evaluates output variability by varying one input parameter at a time, while all other input parameters are held fixed [14]. In contrast, global sensitivity analysis method evaluates the output

variability by varying all the input parameters [14]. In general, the local method detects the net effects of the single parameters, while the global method detects the interaction effects between the different parameters [15, 25].

However, local method is the simplest form of sensitivity analysis and, due to its convenient use, implementation, low computational cost, and is less time-consuming [12, 26], it has been widely and successfully used for building performance analysis [14, 25, 27-29]. On the other hand, local sensitivity analysis method can directly provide a first prediction on the effect of perturbation of the design parameters; hence, it performs an initial assessment of which parameters that have the greatest effect on the model output [30, 31]. Thus, the local method was adopted for the sensitivity analysis in this study.

Despite the previous studies [5, 8] have performed a preliminary sensitivity analysis of the behaviour of the BIPV/T-DSF, only limited design parameters were assessed under a single climatic condition. In this paper, a thorough sensitivity analysis adopting the local method was carried out to evaluate how the model outputs – building energy consumption and indoor thermal comfort – were sensitive to the variations of multiple design parameters of the BIPV/T-DSF for an office building in various climate zones across Australia.

2. Methodology

This study was pursued by using the validated TRNSYS (a building simulation program) models from our previous studies [5, 8-10]. All the necessary design parameters (the input parameters) to be studied were determined prior to the sensitivity analysis. In general, there are substantial design parameters that would potentially affect the building performance on indoor thermal comfort and energy consumption. These usually include the occupancy (operating hours), internal building thermal loads (heat gains from occupants, lighting and appliance), building fabric (for example, walls, floors, roofs, windows and doors that lead to heat transfer between the indoor and outdoor spaces) and air-conditioning systems of the building. The present study is devoted to the understanding of the sensitivity of the design parameters of the BIPV/T-DSF itself on building energy consumption and indoor thermal comfort, so the interventions of the occupancy, internal building thermal loads, air-conditioning systems and building fabric (except the portion of the BIPV/T-DSF in this study) were not considered, which were assigned with fixed values based on the typical settings of office buildings and compliant with Australian building regulations (Table 1). In addition, the orientation of the proposed BIPV/T-DSF model was set facing north, as the solar panels should ideally face in a northerly direction for optimum sun exposure in the southern hemisphere locations.

Table 1. Input values of the fixed design parameters in TRNSYS models.

Parameters	NoVent-DSF	NatVent-DSF	MechVent-DSF	Criteria
Operating hours	8 am to 6 pm	8 am to 6 pm	8 am to 6 pm	Typical settings for offices
Heat gain from occupants	150 W per person	150 W per person	150 W per person	Typical values for offices
Heat gain from computers	25 W/m^2	25 W/m^2	25 W/m^2	Typical values for offices
Heat gain from artificial lighting	5 W/m^2	5 W/m^2	5 W/m^2	Typical values for offices
U-value of external wall	0.51 W/m^2K	0.51 W/m^2K	0.51 W/m^2K	Comply with the Building Code of Australia for office buildings [32]: $U \leq 2.0$ W/m^2K
U-value of external roof	0.24 W/m^2K	0.24 W/m^2K	0.24 W/m^2K	Comply with the Building Code of Australia for office buildings [32]: Climate zone 1, 2, 3, 4, 5 & 7: $U \leq 0.27$ Climate zone 6: $U \leq 0.31$ Climate zone 8: $U \leq 0.21$
Floor – a slab on ground (boundary condition)	Adiabatic	Adiabatic	Adiabatic	Deemed as an adiabatic surface

Three representative climate zones in Australia were chosen for the present study, and their characteristics and weather files used in the simulation are given in Table 2. A single room office building (we considered only one person sitting in the room) configured BIPV/T-DSF with three configurations (as shown in Figure 2) were modelled in TRNSYS that reflecting different modes of ventilation – Non-Ventilated DSF (NoVent-DSF), Naturally-Ventilated DSF (NatVent-DSF) and Mechanically-Ventilated DSF (MechVent-DSF), which are further specified in Table 3. It should be noted that Figure 2 showing the fan in the middle of the cavity for the MechVent-DSF model is an idealised schematic diagram, which might not be a design of the fan allocation in reality. In addition, the dimensions of the three façade/building models are given in Table 4, and a Perovskite-based semi-transparent PV glazing (Table 5) based on the published articles [33, 34], as the external window glazing, was applied to the three models. In order to maximise PV production and compensate the indoor environment for the conceivable shortage of daylighting through the semi-transparent PV glazing, the dimensions of the external (PV glazing) and internal windows were maximised. Consequently, window-to-wall ratio (WWR) was not considered a design parameter in this study, but we will take into consideration that the correlations between the WWR and indoor thermal comfort and energy consumption for the BIPV/T-DSF building in future study.

Table 2. Description of the selected climate zones and weather files.

Location	Climate zone classifications based on Australian Building Codes Board	Weather files used in simulations
Darwin	High humidity summer and warm winter (Climate zone 1)	AUS_NT.Darwin.941200_IWEC.epw
Sydney	Warm temperate (Climate zone 5)	AUS_NSW.Sydney.947670_IWEC.epw
Canberra	Cool temperate (Climate zone 7)	AUS_ACT.Canberra.949260_IWEC.epw

Table 3. Specifications of the three BIPV/T-DSF configurations.

Ventilation mode	Specifications
NoVent-DSF	All ventilation louvres and internal and external windows of the DSF were closed, hence there was no air exchange between the outdoor environment, the cavity and the room; and no ventilation happened within the air cavity.
NatVent-DSF	All the windows and the internal ventilation louvres were closed, hence there was no air exchange between the air cavity and the room. The external ventilation louvres were opened to drive the air exchange between the air cavity and outdoor environment through stack effect.
MechVent-DSF	All the windows and the internal ventilation louvres were closed, hence there was no air exchange between the air cavity and the room. The external ventilation louvres were opened to allow the air exchange between the air cavity and outdoor environment driven by a supply fan, which was located in the air cavity.

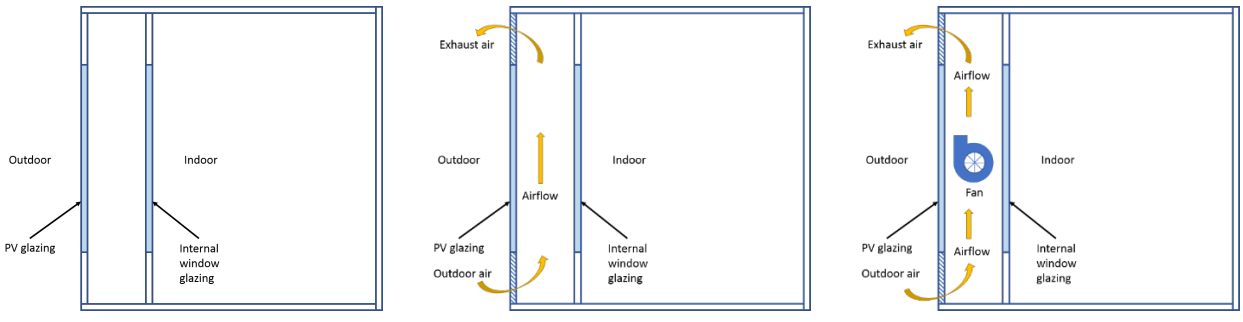

(1) NoVent-DSF (2) NatVent-DSF (3) MechVent-DSF

Figure 2. Schematic diagram of the three façade/building models [5, 8].

Table 4. Dimensions of the three façade/building models.

Parameters	NoVent-DSF	NatVent-DSF	MechVent-DSF
Width of the building	2.44 m	2.44 m	2.44 m
Depth of the building	2.3 m	2.3 m	2.3 m
Height of the building	2.47 m	2.47 m	2.47 m
Width of external window (PV glazing)	2.32 m	2.32 m	2.32 m
Height of external window (PV glazing)	1.3 m	1.3 m	1.3 m
Width of internal window	2.32 m	2.32 m	2.32 m
Height of internal window	1.3 m	1.3 m	1.3 m
Width of the DSF	2.44 m	2.44 m	2.44 m
Depth of the DSF	0.4 m	0.4 m	0.4 m
Height of the DSF	2.47 m	2.47 m	2.47 m
Width of louvre (opening)	N/A	2.32 m	2.32 m
Height of louvre (opening)	N/A	0.5 m	0.5 m

Table 5. Properties of the adopted Perovskite-based semi-transparent PV glazing.

Parameters	Values
U-value	5.59 W/m^{2}K
Visible Light Transmittance (VLT)	37.5%
Solar Transmittance (front)	33.2%
Solar Transmittance (back)	33.2%
Solar Reflectance (front)	3.5%
Solar Reflectance (back)	3.5%
Visible Light Reflectance (front)	4.0%
Visible Light Reflectance (back)	4.0%
Emissivity	0.89
PV efficiency (under STC), η	6.64%
Temperature coefficient of power, α_P	-0.3%/°C

The following design parameters in Table 6 reflect their effects on the efficiency of the DSF, which were chosen for the sensitivity analysis and were varied by applying a range of variations to the original value of the reference model (that is, the BIPV/T-DSF model we assessed in the previous studies [5, 8]). Thermal Transmittance (U-value) measures how much non-solar heat is transferred through an assembly (such as a wall or window), while Solar Heat Gain Coefficient (SHGC) measures how much solar radiation caused heat is transferred through a window. The significant effects of U-value and SHGC on building energy consumption as well as indoor thermal comfort have been demonstrated in previous research [35-37]. Research also demonstrates that the cavity depth of the DSF affects building performance and embodies in the effect of conductive heat transfer and stuck effect of the DSF [38, 39]. Further, research has demonstrated the opening areas for the cavity's natural ventilation and the air exchange rate of the forced ventilation reflect into the DSF's thermal performance in controlling the solar heat gain, and consequently affecting indoor thermal comfort and energy consumption of the building [40-42]. It should be noted that the electric power and useful thermal energy from the BIPV/T-DSF were not deemed to be the design parameters in this study, as only one type of PV glazing was used throughout the study.

Table 6. Design parameters for sensitivity analysis.

Model configuration	Design parameters	
All the three models	- Thermal transmittance of internal window of the DSF	(U_{in})
	- Thermal transmittance of external window of the DSF	(U_{out})
	- Solar heat gain coefficient of internal window of the DSF	($SHGC_{in}$)
	- Solar heat gain coefficient of external window of the DSF	($SHGC_{out}$)
	- Cavity depth of the DSF	(D_{ca})
MechVent-DSF model	- Air exchange rate of the supply fan	(Q_{ACH})
NatVent-DSF model	- Louvre's opening ratio of the DSF (discharge coefficient[1])	(C_L)

Basically, the form of the design parameters could be categorised into two groups, which are geometry and auxiliary (that is, D_{ca}, Q_{ACH} and C_L) and material (that is, U_{in}, U_{out}, $SHGC_{in}$ and $SHGC_{out}$). As a result, it can simplify the analysis and demonstrate which category of the design parameter is more influential for the performance of the façade/building. The selected design parameters and their ranges of variations and original values (the reference model values) are given in Table 7. It should be noted that the both opaque portions of the external and internal walls of the BIPV/T-DSF were not chosen for the sensitivity analysis as the windows comprised most of the surface area, which means the opaque portions were considered the minor influential factors. As can be seen in Table 7, in order to simplify the comparison of the sensitivity among the different parameters, the variations of all design parameters were expressed by percentage values. Due to the manufacturer's information for the perturbation of SHGC and U-value of the PV glazing was not available, a normal external window with a range of SHGC and U-value was chosen to analyse the sensitivity of the outer layer of the BIPV/T-DSF. The external window with the complete data of glazing in the TRNSYS window library based on the International Glazing Database, which contains the detailed spectral optical and thermal data for more than 1,000 glazing products from manufacturers.

Table 7. Variation ranges and original values of the design parameters for sensitivity analysis.

Parameter	Unit	Original value	Range of variation[2]	Interval of variation
U_{in}	W/m^2K	5.68	-75% to +3%	N/A
U_{out}	W/m^2K	2.35	-46% to +29%	N/A
$SHGC_{in}$	-	0.86	-50% to +1%	N/A
$SHGC_{out}$	-	0.624	-30% to +30%	±10%
D_{ca}	m	0.4	-60% to +60%	±20%
Q_{ACH}	ACH	400	-60% to +60%	±20%
C_L	-	0.39	-30% to +30%	±10%

As mentioned earlier, the sensitivity analysis of the present study was aimed at evaluating which design parameters are both the indoor thermal comfort and energy consumption of the BIPV/T-DSF building significantly sensitive to. To this objective, a "Sensitivity Index (SI)" was used to determine the sensitivity of the selected design parameters, which can be calculated as follows [14]:

$$SI = \frac{E_{max} - E_{min}}{E_{max}} \times 100\% \quad (1)$$

[1] In this study, the louvre's opening ratio was implemented by modulating a discharge coefficient, which is the ratio of the actual airflow to the theoretical airflow.

[2] The negative percentage denotes the reduction of the value of the parameter, while the positive percentage denotes the increase of the value of the parameter.

Where E_{max} and E_{min} are the maximum and minimum output values (i.e. indoor thermal comfort or energy consumption) respectively, which are used to calculate the output difference in percentage (%) of the two extreme values – the maximum and minimum ones – of the design parameter by varying it over its entire range of the variation [14].

All sensitivity indices of the corresponding design parameters were then ranked qualitatively and the most important design parameters were determined accordingly. In this study, the first three ranks from the selected seven design parameters were deemed to be the most important design parameters, which basically included all parameters within the higher half of the set of the seven sensitivity indices (correspond to the seven design parameters); this was based on a statistical theory of the median position, which represents the central importance in robust statistics and it avoids determining the parameter's importance arbitrarily [43]. In future study, the most important design parameters are optimised in order to achieve the optimisation of building performances, while the unimportant design parameters that have minor impact on the building performances would be considered keeping the original characteristics hence improve the efficiency of the design processes [14].

Prior to calculating the SI, energy consumption and indoor thermal comfort of the BIPV/T-DSF building models must be determined numerically. Energy consumption can be easily calculated based on an energy balance mathematical model of the Type56 (the building model) in TRNSYS using the following equations [44, 45]:

$$q_{s,i} = q_{comb,s,i} + S_{s,i} + Wallgain \quad (2)$$

$$q_{s,o} = q_{comb,s,o} + S_{s,o} \quad (3)$$

Where $q_{s,i}$ is the conductive heat flux from the wall at the inside surface, $q_{s,o}$ is the conductive heat flux into the wall at the outside surface, $q_{comb,s,i}$ is the combined convective and radiative heat flux in the space, $q_{comb,s,o}$ is the combined convective and radiative heat flux to the surface, $S_{s,i}$ is the both solar radiation and long-wave radiation generated from internal objects (e.g. occupants, furniture and appliance), $S_{s,o}$ is the solar radiation from external surfaces, *Wallgain* is a user-defined energy flow to the surfaces of inside wall or window.

Further, for the calculation of the energy consumption, a reversible heat pump system with a heating coefficient of performance (COP) of 3.5 and cooling COP of 2.5 was modelled in the proposed building model as per the previous study [5], which provided heating and cooling for the building in maintaining the setpoint temperatures. In this study, the setpoint temperature for heating and cooling were 22°C and 26°C respectively.

Comparing with energy consumption, the evaluation of indoor thermal comfort is more complicated as indoor thermal comfort is subjectively different for every individual. Accordingly, we adopted the adaptive comfort standard of ASHRAE 55 [46] to determine the acceptability of indoor conditions in free-running buildings (therefore, in this study, the air-conditioning systems were not in operations when evaluating the indoor thermal comfort) given the seven days' weighted mean outdoor air temperature (the average of the previous seven days' daily average outdoor air temperatures) and the indoor operative temperature by comparing the hourly values of the operative temperature with comfort limits [46]. Any hours of the operative temperature outside the comfort limits are deemed to be discomfort hours. Finally, whole year discomfort hours (including both the cooling and heating discomfort hours) were calculated accordingly and used to evaluate the indoor thermal comfort.

TRNFlow, an external plugin, was chosen for the integration with the TRNSYS thermal building model for modelling airflow in the DSF cavity. Based on our previously published work [5], an airflow network of the ventilated building model were created in terms of the selected airlinks – DSF and outdoor air in this study – in TRNFlow. Basically, the airflow models between the selected airlinks were modified accordingly. In detail, both the external air and DSF were linked together, in which the ventilation louvres were modelled as large opening (which is the most fit type of link for modelling the ventilation louvres in TRNFlow).

3. Results

In this section, the sensitivity and correlation between the simulation outputs (i.e. indoor thermal comfort and energy consumption) and the input parameters were analysed, which show how important the input parameters for the different configurations (NoVent-DSF, NatVent-DSF and MechVent-DSF) of the BIPV/T-DSF under the three selected climate zones (Darwin, Sydney and Canberra) respectively. In the analysis, the values of the selected design parameters (the input values) were varied within the given range of variations, and the effect of the variations on the output values (represented by discomfort hours and energy consumption) was evaluated based on the TRNSYS simulation results. As mentioned earlier, energy consumption was directly calculated in TRNSYS and the whole year energy consumption was presented as the output value quantifying the energy performance, while the whole year discomfort hours were used to present the output value quantifying indoor comfort performance.

3.1. Correlation analysis for the high humidity summer and warm winter climate case

As shown in Figure 3, the vertical axis show the variation of discomfort hours or energy consumption in percentage (the positive and negative percentage mean the increase and reduction in discomfort hours or energy consumption, respectively) against the variations of the design parameters (in percentage along the horizontal axis) in the corresponding ventilation mode under the climate of high humidity and warm winter (represented by Darwin). As can be seen, varying the U-value for internal window (U_{in}) of the DSF led to a significant change on both the discomfort hours and energy consumption. The variations of discomfort hours and energy consumption were basically symmetric when varying the U_{in}, in which the discomfort hours increased almost linearly with the decrease of the U_{in}, however, which was the opposite for energy consumption. On the other hand, although the declines of energy consumption were similar among the three models, the slopes of discomfort hours against U_{in} of the two ventilated models were almost twice as higher as that of the non-ventilated model. By comparison, the variation of U-value of the external window (U_{out}) did slightly change the outputs, which represented as a linear correlation that both the decrease of discomfort hours and energy consumption with the increase of U_{out}. This reflects, in Darwin, that the indoor comfort and energy consumption are even more directly tied to thermal transmittance of the internal window. To interpret the phenomenon of the inverse relation between thermal transmittance and the outputs, thermal transmittance of a window reflects the ability to prevent heat transmission between outside and inside of a building; thermal insulation of the window was enhanced accordingly with the decrease of the thermal transmittance, which diminished the heat transmission between the outdoor and indoor environments hence reduced the energy consumption for space conditioning. On the contrary, the discomfort hours were being increased by reducing the U_{in} due to the accumulating of overheat in the free-running room under such hot climatic condition in Darwin.

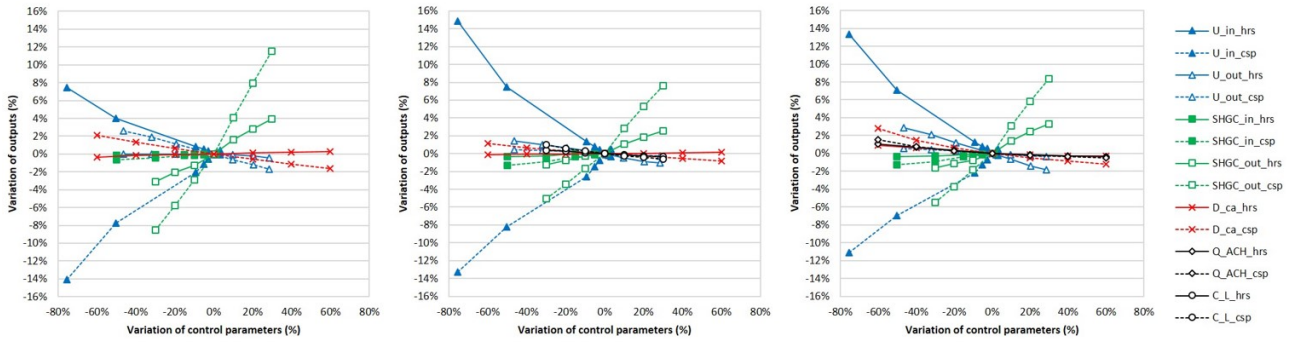

Figure 3. Variation of discomfort hours (solid lines with the suffix "hrs") and energy consumption (dotted lines with the suffix "csp") on an annual basis – Darwin. NoVent-DSF model (left), NatVent-DSF model (middle), MechVent-DSF model (right).

The outputs were proportional to the perturbation of SHGCs of the both windows of the DSF, of which the outputs were linearly increasing with the increase of the SHGCs. Although the perturbation of SHGC of the internal window ($SHGC_{in}$) had a limited effect on the changes of outputs, perturbing the SHGC of the external window ($SHGC_{out}$) produced a degree

of impact on discomfort hours and markable impact on energy consumption for all the three models, especially for the NoVent-DSF the energy consumption was being significantly increased by increasing the $SHGC_{out}$. This, however, reflects the building's indoor thermal comfort and energy consumption (under the high humidity summer and warm winter climate) were highly sensitive to $SHGC_{out}$ rather than $SHGC_{in}$.

It was also found that varying the cavity depth (D_{ca}) produced the similar outputs variation patterns for all the three models. In this case, energy consumption was being reduced linearly by increasing the depth of the air cavity, but varying cavity depth made a negligible change on discomfort hours. In theory, this can be interpreted as the increase of cavity depth made the decrease of conductive heat transfer between the outdoor and indoor spaces and therefore a reduction of energy demand. Generally, the outputs were less sensitive to D_{ca}.

Moreover, in terms of a linear trend, the output values (discomfort hours and energy consumption) were inversely proportional to the values of the ventilation louvres' opening ratio (C_L) and the fan air exchange rate (Q_{ACH}) for the NatVent-DSF and MechVent-DSF models, respectively. The observably slight fluctuation of the curves indicated the outputs were not greatly sensitive to both the C_L and Q_{ACH}, which also reflected that the overheat issue in the air cavity in Darwin could not be mitigated easily by strengthening the cavity ventilation.

3.2. Correlation analysis for the warm temperate climate case

According to the results are shown in Figure 4, it is seen that the variations of most of the design parameters affected the outputs of the corresponding models in a linear trend under the warm temperate climate (represented by Sydney). In particular, the perturbation of $SHGC_{out}$ always made a significant change of the output values of the three models especially for the change of energy consumption, which presented as the output values were proportional to the value of $SHGC_{out}$. Similarly, the changes of the output values were also proportional to the change of $SHGC_{in}$, but the perturbation of the $SHGC_{in}$ barely affected the changes of the output values for the three models especially for the NoVent-DSF model. Thus, similar to the case of Darwin, the building's indoor thermal comfort and energy consumption in Sydney were also highly sensitive to $SHGC_{out}$ but less sensitive to $SHGC_{in}$.

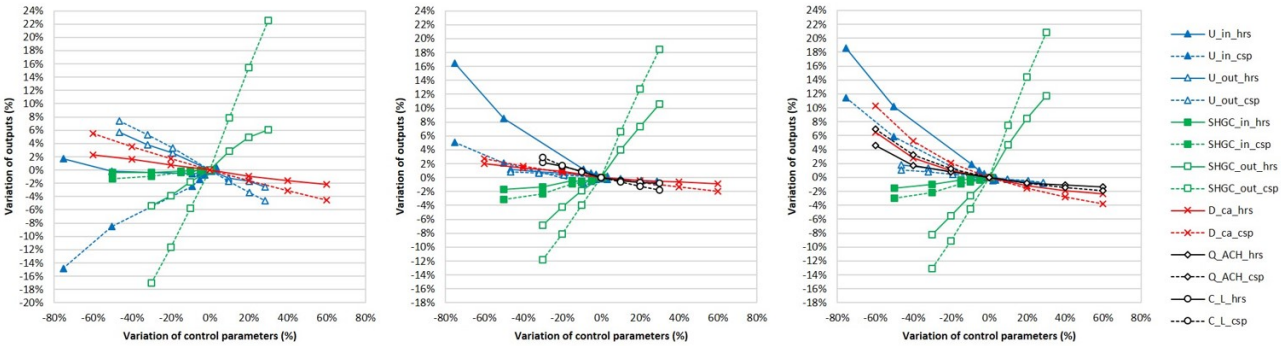

Figure 4. Variation of discomfort hours (solid lines with the suffix "hrs") and energy consumption (dotted lines with the suffix "csp") on an annual basis – Sydney. NoVent-DSF model (left), NatVent-DSF model (middle), MechVent-DSF model (right).

It can be seen that the discomfort hours were being increased by reducing the U_{in} for all the three models, which even led to the more significant changes for that of the two ventilated models. From the energy perspective, the energy consumption was being reduced by reducing U_{in} for the NoVent-DSF, while the two ventilated models had the opposite effects. As having the lower thermal transmittance in the warm temperate climate, the building is not better in transmitting excessive heat gains to the outdoor environments and therefore results in more discomfort hours and consequently a higher energy demand, especially for the ventilated DSF more extra heat is being trapped in the cavity through the ventilation between the cavity and outdoors. Similarly, the output values were increased with the decrease of U_{out}, but this parameter had more impact on the non-ventilated model, while less impact on the two ventilated models, which was probably due to the

improved cooling effect of the external window through the twofold ventilations on both sides of the window; and this indirectly led to the bifold effects of U_{in} on energy consumption variations for the non-ventilated and ventilated models.

Also, perturbing the value of D_{ca} had a degree of impact on the output values in terms of an inversely proportional relation. In this case, outputs of the NoVent-DSF and MechVent-DSF were more sensitive to D_{ca}, which reflected that the geometric effects of the cavity were more subject to the stable environments of the air movement. Further, compare with the Darwin case, it can be noticed that both the C_L and Q_{ACH} had the larger effects on the outputs for the corresponding ventilated models under the cooler climatic condition (Sydney), and the lesser discomfort hours and energy consumption were being achieved by enhancing the ventilation in the cavity.

3.3. Correlation analysis for the cool temperate climate case

Looking at Figure 5, the influences of most of the design parameters on the output values for the different DSF models were almost linear under the cool temperate climate (represented by Canberra). Both the variations of U_{in} and $SHGC_{out}$ significantly affected the variations of discomfort hours for the three DSF models, and the energy consumptions were even more sensitive to the variations of the two parameters (U_{in} and $SHGC_{out}$) as reflected in the large extent of variations of the corresponding curves especially for the NoVent-DSF model.

Basically, the output values were proportional to the value of the U_{in} and $SHGC_{out}$ except for the variations of discomfort hours against $SHGC_{out}$ for the ventilated models. In the MechVent-DSF model the curve of $SHGC_{out}$ was symmetrically distributed around the original value and the discomfort hours were being increased when the $SHGC_{out}$ either being increased or decreased; however, increasing $SHGC_{out}$ always produced the increase of energy consumption, which was similar to the Sydney's case. In the NatVent-DSF model the $SHGC_{out}$ curve converged towards the symmetrical distribution around the point of -10% and the discomfort hours started increasing at this point towards the two sides of the ordinate, but the energy consumption was being increased with the increase of $SHGC_{out}$. This phenomenon, however, was possibly due to the algorithm of the total discomfort hours, which was the sum of the cooling and heating discomfort hours, and their variation rates were largely different from one another and this was particularly noticeable in the cool temperate climate; while the variation intervals of the energy consumption were basically stable in this case. In comparison, the variation of $SHGC_{in}$ had a very limited effect on the variation of the outputs for the three models.

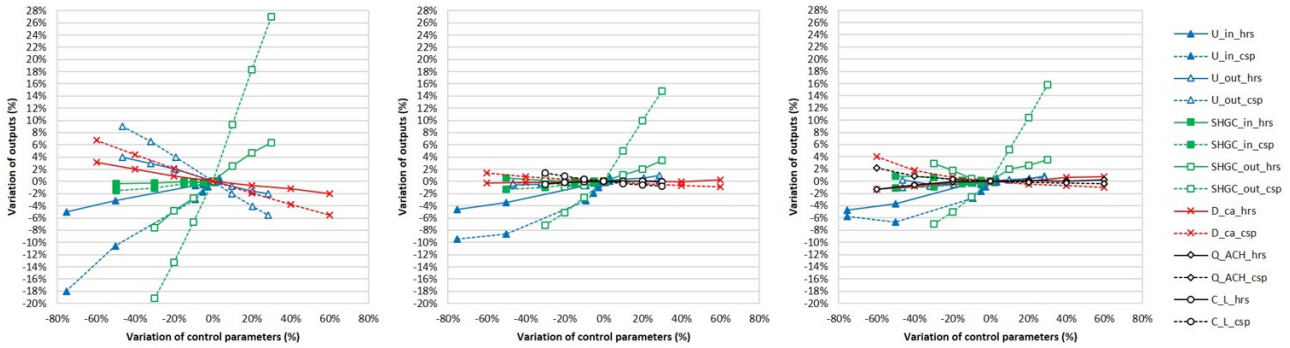

Figure 5. Variation of discomfort hours (solid lines with the suffix "hrs") and energy consumption (dotted lines with the suffix "csp") on an annual basis – Canberra. NoVent-DSF model (left), NatVent-DSF model (middle), MechVent-DSF model (right).

Comparing to the case in Sydney, the impact of trapping heat by the lower thermal transmittance window in the colder climate (Canberra) is largely diminished, and therefore it was found that the decrease of the discomfort hours and energy consumption with the decrease of U_{in} in Canberra (note: $U_{\_in\_csp}$ at -75% for MechVent-DSF was an exception due to the algorithm of the total energy consumption). Also, in Canberra, the output values of the NoVent-DSF model were markedly sensitive to U_{out} and D_{ca}, and the variation trends of the corresponding curves were close to that of Sydney. However, the outputs of the two ventilated models were not that sensitive to U_{out} and D_{ca}.

In addition, the variations of other parameters, such as the louvres' opening ratio (C_L) and the fan air exchange rate (Q_{ACH}), barely made changes on either discomfort hours or energy consumption for the corresponding ventilated models in Canberra; and this reflected that the ventilation in the air cavity was a minor factor in relation to both the indoor thermal comfort and energy consumption of the building in the cool temperate climate. It was presumed that the ventilation factor within the DSF's cavity had the greater effect on building energy efficiency and thermal comfort for the warm temperate climate than that of the more extreme climates (e.g. cool temperate climate and hot all year-round climate).

4. Discussion

According to the results presented in the previous section, the correlations between most of the design parameters and their corresponding simulation outputs (discomfort hours and energy consumption) were almost linear trends, which made the impact of variation comparable in the whole parameter range. In order to quantify the significance of the selected design parameters, a ranking of the importance of the design parameters to the outputs was examined by introducing the Sensitivity Index (SI) aforementioned.

4.1. Importance of design parameters to simulation outputs – the high humidity summer and warm winter climate

The SI for each of the design parameters corresponds to the respective simulation outputs – indoor thermal comfort and energy consumption – are presented in Figure 6 for the three BIPV/T-DSF models under the high humidity summer and warm winter climate (Darwin). Fundamentally, the higher the SI value the more important the design parameter to the outputs. Looking at the bar plots in Figure 6, both U_{in} and $SHGC_{out}$ showed the highest SI in regard to indoor thermal comfort and energy consumption for all the three models (most of the SI values were above 10%), while the other design parameters showed the less SI and most of them were below 5%.

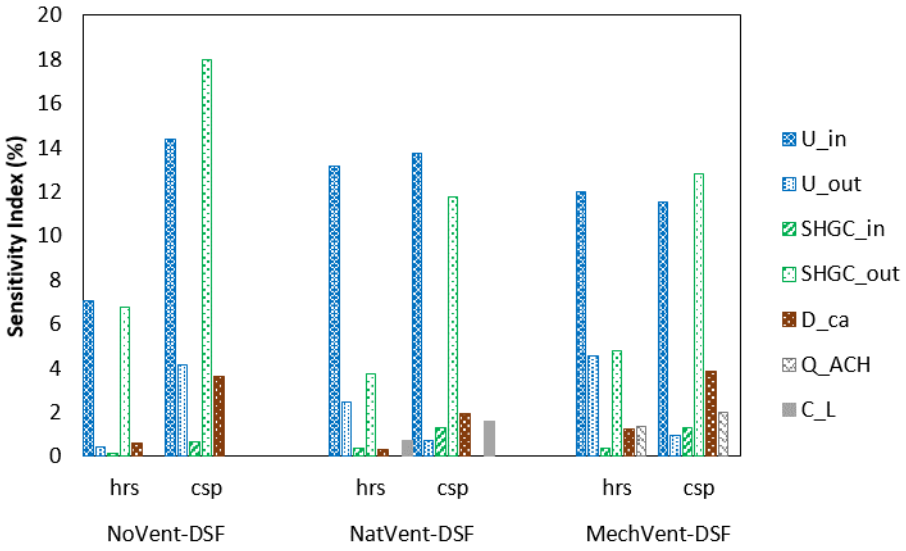

Figure 6. Sensitivity indices for design parameters correspond to indoor thermal comfort (hrs) and energy consumption (csp) – Darwin.

Further, the ranking of the design parameters' importance to the simulation outputs for Darwin is listed in Table 8 in order to evaluate the importance numerically. Based on the ranking, it can be concluded that the design parameters related to thermal insulation of the internal window (represented by U_{in}) and solar heat transmission of the external window (represented by $SHGC_{out}$) of the BIPV/T-DSF had the highest SI (always in the top two position) for the different models and therefore they were the most important design parameters to indoor thermal comfort and energy consumption. Thermal insulation of the external window (represented by U_{out}) also had the notable importance to indoor thermal comfort,

especially for the ventilated models. In addition, according to the ranking, cavity depth of the DSF (D_{ca}) had a limited effect on energy consumption for the NoVent-DSF model but a degree of effect on that of the two ventilated models. Basically, the most important design parameters were identified in line with the first three ranks method defined in the Methodology section.

Table 8. Ranking of design parameters' importance to indoor thermal comfort (hrs) and energy consumption (csp) – Darwin.

Design parameter	NoVent-DSF				NatVent-DSF				MechVent-DSF			
	SI (%) *hrs*	Rank *hrs*	SI (%) *csp*	Rank *csp*	SI (%) *hrs*	Rank *hrs*	SI (%) *csp*	Rank *csp*	SI (%) *hrs*	Rank *hrs*	SI (%) *csp*	Rank *csp*
U_{in}	7.03	1	14.39	2	13.18	1	13.74	1	11.97	1	11.54	2
U_{out}	0.45	4	4.15	3	2.45	3	0.74	6	4.57	3	0.93	6
$SHGC_{in}$	0.14	5	0.63	5	0.37	5	1.30	5	0.36	6	1.27	5
$SHGC_{out}$	6.75	2	17.96	1	3.75	2	11.79	2	4.77	2	12.78	1
D_{ca}	0.60	3	3.65	4	0.28	6	1.93	3	1.23	5	3.87	3
Q_{ACH}	-	-	-	-	-	-	-	-	1.35	4	1.97	4
C_L	-	-	-	-	0.70	4	1.57	4	-	-	-	-

4.2. Importance of design parameters to simulation outputs – the warm temperate climate

Figure 7 shows the bar plots of the SI that quantifying the correlations between the design parameters and the simulation outputs (indoor thermal comfort and energy consumption) for the respective BIPV/T-DSF models under the warm temperate climate (Sydney). Apparently, both U_{in} and $SHGC_{out}$ had the significantly higher SI for most of the cases, especially the SI of U_{in} for discomfort hours of the NatVent-DSF model reached the highest value (about 43%); and $SHGC_{out}$ also showed the relatively higher SI for energy consumption of the three models (all the SI values exceeded 25%). D_{ca} was another parameter had the noticeable value of the SI for NoVent-DSF and MechVent-DSF models, and most of the SI values were nearly or above 5% for discomfort hours and around 10% for energy consumption.

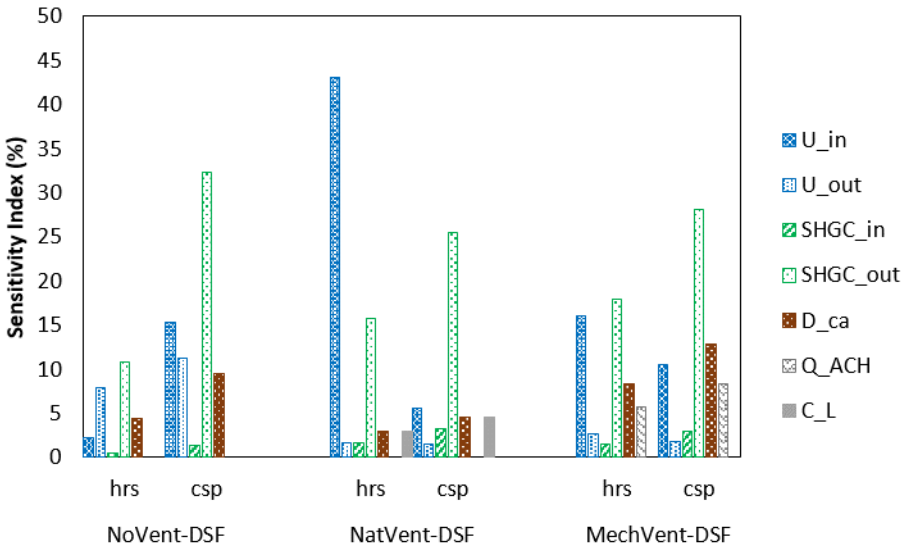

Figure 7. Sensitivity indices for design parameters correspond to indoor thermal comfort (hrs) and energy consumption (csp) – Sydney.

Table 9 shows the ranking of the design parameters' importance to indoor thermal comfort and energy consumption of the different BIPV/T-DSF configurations for Sydney. Based on the ranking the SI for $SHGC_{out}$ was always higher than the other parameters regarding energy consumption for all the model configurations and considered the most important design

parameter in this case. $SHGC_{out}$ also showed the highest importance to indoor thermal comfort for the NoVent-DSF and MechVent-DSF models. In addition, U_{in} was another important parameter for indoor thermal comfort for the two ventilated models especially the SI took the first place for the NatVent-DSF model; while U_{out} showed importance to the outputs of the NoVent-DSF model, of which the SI took the second place for discomfort hours and third place for energy consumption. U_{in} was also an important design parameter within the first three ranks affecting building energy consumption for the three DSF models in Sydney. Moreover, cavity depth (D_{ca}) was considered an important parameter for the MechVent-DSF model based on its SI value, which had the second highest SI for energy consumption and the third highest SI for discomfort hours; and D_{ca} also had the importance in the third place to discomfort hours of the NoVent-DSF model and energy consumption of the NatVent-DSF model, respectively.

Table 9. Ranking of design parameters' importance to indoor thermal comfort (hrs) and energy consumption (csp) – Sydney.

Design parameter	NoVent-DSF				NatVent-DSF				MechVent-DSF			
	SI (%) *hrs*	Rank *hrs*	SI (%) *csp*	Rank *csp*	SI (%) *hrs*	Rank *hrs*	SI (%) *csp*	Rank *csp*	SI (%) *hrs*	Rank *hrs*	SI (%) *csp*	Rank *csp*
U_{in}	2.29	4	15.25	2	43.13	1	5.54	2	16.04	2	10.45	3
U_{out}	7.82	2	11.18	3	1.71	5	1.43	6	2.60	5	1.73	6
$SHGC_{in}$	0.41	5	1.32	5	1.71	5	3.17	5	1.53	6	2.99	5
$SHGC_{out}$	10.75	1	32.30	1	15.77	2	25.54	1	17.87	1	28.09	1
D_{ca}	4.33	3	9.47	4	2.91	4	4.58	3	8.27	3	12.82	2
Q_{ACH}	-	-	-	-	-	-	-	-	5.64	4	8.27	4
C_L	-	-	-	-	2.96	3	4.51	4	-	-	-	-

4.3. Importance of design parameters to simulation outputs – the cool temperate climate

Figure 8 shows the bar plots of the SI for the correlations between the design parameters and simulation outputs for the three models under the cool temperate climate (Canberra). It is seen that $SHGC_{out}$ had the highest SI values corresponding to energy consumption for the three models, and all the SI were higher than 19% and the SI value for NoVent-DSF model was even higher than 35%. Regarding the discomfort hours, $SHGC_{out}$ also had the distinctly higher SI values for the three models, especially had an SI value of 13% approximately for the NoVent-DSF model. U_{in} also had the relatively higher SI values for the three models, which basically reached the SI value about 5% for discomfort hours for all models and reached even the higher SI values corresponding to energy consumption (about 18%, 10% and 7% for NoVent-DSF, NatVent-DSF and MechVent-DSF, respectively). Besides, D_{ca} and U_{out} had also the comparably higher SI for the NoVent-DSF model and the SI values reached around 5% for discomfort hours and 12% for energy consumption.

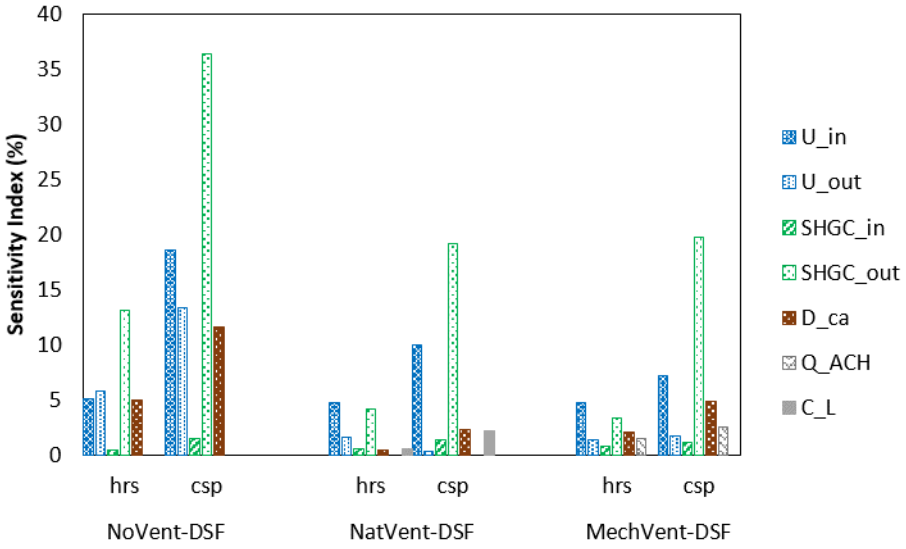

Figure 8. Sensitivity indices for design parameters correspond to indoor thermal comfort (hrs) and energy consumption (csp) – Canberra.

According to the SI ranking in Table 10, $SHGC_{out}$ held the first rank of the SI for both the discomfort hours and energy consumption for the NoVent-DSF model, which also held the first and second ranks of the SI for energy consumption and discomfort hours respectively for the ventilated models. In addition, the SI values for U_{in} always occupied the first three ranks for the three models, and particularly marked for the two ventilated models which held the first and second places for discomfort hours and energy consumption respectively. Also, the SI for U_{out} was within the first three ranks for the outputs of the NoVent-DSF model and took the third place for discomfort hours of the NatVent-DSF model. Further, D_{ca} had the SI reached the third place for energy consumption of the NatVent-DSF model and for the both outputs (discomfort hours and energy consumption) of the MechVent-DSF model. All the above described design parameters were deemed to be the most important ones for the corresponding BIPV/T-DSF cases in Canberra.

Table 10. Ranking of design parameters' importance to indoor thermal comfort (hrs) and energy consumption (csp) – Canberra.

Design parameter	NoVent-DSF				NatVent-DSF				MechVent-DSF			
	SI (%) *hrs*	Rank *hrs*	SI (%) *csp*	Rank *csp*	SI (%) *hrs*	Rank *hrs*	SI (%) *csp*	Rank *csp*	SI (%) *hrs*	Rank *hrs*	SI (%) *csp*	Rank *csp*
U_{in}	5.03	3	18.54	2	4.66	1	10.00	2	4.69	1	7.20	2
U_{out}	5.74	2	13.35	3	1.54	3	0.33	6	1.30	5	1.68	5
$SHGC_{in}$	0.37	5	1.51	5	0.55	4	1.34	5	0.80	6	1.16	6
$SHGC_{out}$	13.07	1	36.38	1	4.14	2	19.12	1	3.36	2	19.66	1
D_{ca}	4.95	4	11.54	4	0.46	6	2.22	3	2.07	3	4.80	3
Q_{ACH}	-	-	-	-	-	-	-	-	1.45	4	2.56	4
C_L	-	-	-	-	0.51	5	2.18	4	-	-	-	-

5. Conclusions

Sensitivity Analysis plays a valuable role in identifying the effect of the variations of the design parameters on building performances in the early stage of the design processes; therefore, the late stage of building design and optimisation is more efficient and structured by focusing on the fewer parameters with high importance. In this study, local method was

adopted to perform the proposed sensitivity analysis. The sensitivity analysis provided a thorough prediction on the effect of the variations of the design parameters of a BIPV/T-DSF on the performance of indoor thermal comfort and energy consumption for an office building. In terms of the forms, the design parameters were categorised as two groups in this study:

- geometry and auxiliary (D_{ca}, Q_{ACH} and C_L); and
- material (U_{in}, U_{out}, $SHGC_{in}$ and $SHGC_{out}$).

The sensitivity analysis presented in this paper showed analytically which design parameters of the BIPV/T-DSF were the most important ones to be refined in order to improving indoor thermal comfort and reducing energy consumption for the proposed BIPV/T-DSF building with different configurations (non-ventilation, natural ventilation and mechanical ventilation) under the various climatic conditions in Australia.

The results of the sensitivity analysis showed that the thermal transmittance of the internal window (U_{in}) and solar heat gain coefficient of the external window ($SHGC_{out}$) were the most important design parameters having the largest influence on both indoor thermal comfort and energy consumption for all the ventilation modes of the BIPV/T-DSF building in the high humidity summer and warm winter climate (represented by Darwin). Also, in the case of Darwin, thermal transmittance of the external window (U_{out}) and cavity depth (D_{ca}) were considered the important design parameters for the BIPV/T-DSF.

In the warm temperate climate (represented by Sydney), $SHGC_{out}$ was the most important parameter for all the BIVP/T-DSF models affecting both indoor thermal comfort and energy consumption, while U_{in} was another one of the most important parameters affecting energy consumption for the three models and indoor thermal comfort for the ventilated models. Besides, U_{out} was crucial for the non-ventilated model in controlling indoor thermal comfort and energy consumption. In addition, D_{ca} was another important parameter for the aspect of indoor thermal comfort of the non-ventilated model, which was also important for the naturally-ventilated model with regard to energy consumption and for the mechanically-ventilated model in controlling both the indoor thermal comfort and energy consumption for the building.

In the cool temperate climate (represented by Canberra), $SHGC_{out}$ was the most important design parameter affecting indoor thermal comfort and energy consumption for the three BIPV/T-DSF models, especially for the non-ventilated one. U_{in} was another important design parameter for the three models regarding the both aspects of indoor thermal comfort and energy consumption. Besides, for the non-ventilated model, U_{out} had a significant influence on indoor thermal comfort and energy consumption as well. Furthermore, D_{ca} was also one of the most important design parameters for the mechanically-ventilated model that affecting the indoor thermal comfort and energy consumption, which was also important in controlling energy consumption of the naturally-ventilated model.

Future research and design are therefore able to concentrate merely on the identified most important design parameters, and consequently simplify the optimisation process of the design of the BIPV/T-DSF under the corresponding design conditions, thus make the well-directed design solution in controlling indoor thermal comfort and energy consumption of the buildings.

It also has to be noted that this study was based solely upon the computer simulation, which remains a challenge even alongside a detailed validation step-by-step for the BIPV/T-DSF models in our previous studies, as any simulation would have a certain degree of error inherently. Therefore, a further verification for both the TRNSYS and TRNFlow simulation results in terms of physical experimentation is required, and this falls within the scope of future study. In addition, the prototype of the BIPV/T-DSF was modelled as an office room, which could not fully represent an office building. This, somehow, limited the research applicability to an actual office building; future study will extend to explore the performance of a multi-story office building with BIPV/T-DSF, and the industry will be benefitted more from that.

Acknowledgments

The authors would like to gratefully acknowledge the financial support for this work provided by the Faculty of Built Environment, University of New South Wales (Australia). The authors would also like to thank Dr. Alessandro Cannavale at Polytechnic University of Bari (Italy) for providing the indispensable data of the Perovskite-based photovoltaic devices.

References

1. Sadineni, S.B., S. Madala, and R.F. Boehm, *Passive building energy savings: A review of building envelope components.* Renewable and Sustainable Energy Reviews, 2011. **15**(8): p. 3617-3631.
2. Yang, T. and A.K. Athienitis, *A review of research and developments of building-integrated photovoltaic/thermal (BIPV/T) systems.* Renewable and Sustainable Energy Reviews, 2016. **66**: p. 886-912.
3. Agathokleous, R.A. and S.A. Kalogirou, *Double skin facades (DSF) and building integrated photovoltaics (BIPV): A review of configurations and heat transfer characteristics.* Renewable Energy, 2016. **89**: p. 743-756.
4. Prieto, A., et al., *COOLFACADE: State-of-the-art review and evaluation of solar cooling technologies on their potential for façade integration.* Renewable and Sustainable Energy Reviews, 2019. **101**: p. 395-414.
5. Yang, S., et al., *Performance assessment of BIPV/T double-skin façade for various climate zones in Australia: Effects on energy consumption.* Solar Energy, 2020. **199**: p. 377-399.
6. Ioannidis, Z., et al., *Modeling of double skin façades integrating photovoltaic panels and automated roller shades: Analysis of the thermal and electrical performance.* Energy and Buildings, 2017. **154**: p. 618-632.
7. Ding, W., Y. Hasemi, and T. Yamada, *Natural ventilation performance of a double-skin façade with a solar chimney.* Energy and Buildings, 2005. **37**(4): p. 411-418.
8. Yang, S., et al., *Numerical simulation study of BIPV/T double-skin facade for various climate zones in Australia: Effects on indoor thermal comfort.* Building Simulation, 2019. **12**(1): p. 51-67.
9. Yang, S., et al., *Studies on Optimal Application of Building Integrated Photovoltaic/Thermal Facade for Commercial Buildings in Australia*, in *Solar World Congress 2017*. 2017: Abu Dhabi, UAE. p. 672-681.
10. Yang, S., et al., *Study of Building Integrated Photovoltaic/Thermal Double-Skin Facade for Commercial Buildings in Sydney, Australia*, in *Final conference of COST TU1403 "Adaptive Facades Network"*. 2018: Lucerne, Switzerland.
11. Yu, J., et al., *Sensitivity analysis of energy performance for high-rise residential envelope in hot summer and cold winter zone of China.* Energy and Buildings, 2013. **64**: p. 264-274.
12. Delgarm, N., et al., *Sensitivity analysis of building energy performance: A simulation-based approach using OFAT and variance-based sensitivity analysis methods.* Journal of Building Engineering, 2018. **15**: p. 181-193.
13. Lomas, K.J. and H. Eppel, *Sensitivity analysis techniques for building thermal simulation programs.* Energy and buildings, 1992. **19**(1): p. 21-44.
14. Heiselberg, P., et al., *Application of sensitivity analysis in design of sustainable buildings.* Renewable Energy, 2009. **34**(9): p. 2030-2036.
15. Bar Massada, A. and Y. Carmel, *Incorporating output variance in local sensitivity analysis for stochastic models.* Ecological Modelling, 2008. **213**(3-4): p. 463-467.
16. Lam, J.C. and S.C.M. Hui, *Sensitivity analysis of energy performance of office buildings.* Building and Environment, 1996. **31**(1): p. 27-39.
17. Garcia Sanchez, D., et al., *Application of sensitivity analysis in building energy simulations: Combining first- and second-order elementary effects methods.* Energy and Buildings, 2014. **68**: p. 741-750.
18. Saltelli, A., S. Tarantola, and F. Campolongo, *Sensitivity anaysis as an ingredient of modeling.* Statistical Science, 2000. **15**(4): p. 377-395.
19. Yang, Z. and B. Becerik-Gerber, *A model calibration framework for simultaneous multi-level building energy simulation.* Applied Energy, 2015. **149**: p. 415-431.
20. Tian, W., *A review of sensitivity analysis methods in building energy analysis.* Renewable and Sustainable Energy Reviews, 2013. **20**: p. 411-419.
21. Tian, W. and P. de Wilde, *Uncertainty and sensitivity analysis of building performance using probabilistic climate projections: A UK case study.* Automation in Construction, 2011. **20**(8): p. 1096-1109.

22. Tian, W., et al., *Bootstrap techniques for sensitivity analysis and model selection in building thermal performance analysis.* Applied Energy, 2014. **135**: p. 320-328.
23. Sreedevi, S. and T.I. Eldho, *A two-stage sensitivity analysis for parameter identification and calibration of a physically-based distributed model in a river basin.* Hydrological Sciences Journal, 2019. **64**(6): p. 701-719.
24. van Griensven, A., et al., *A global sensitivity analysis tool for the parameters of multi-variable catchment models.* Journal of Hydrology, 2006. **324**(1-4): p. 10-23.
25. Spitz, C., et al., *Practical application of uncertainty analysis and sensitivity analysis on an experimental house.* Energy and Buildings, 2012. **55**: p. 459-470.
26. Morio, J., *Global and local sensitivity analysis methods for a physical system.* European Journal of Physics, 2011. **32**(6): p. 1577-1583.
27. Petersen, S. and S. Svendsen, *Method and simulation program informed decisions in the early stages of building design.* Energy and Buildings, 2010. **42**(7): p. 1113-1119.
28. Sun, Y., *Sensitivity analysis of macro-parameters in the system design of net zero energy building.* Energy and Buildings, 2015. **86**: p. 464-477.
29. Kristensen, M.H. and S. Petersen, *Choosing the appropriate sensitivity analysis method for building energy model-based investigations.* Energy and Buildings, 2016. **130**: p. 166-176.
30. Ingalls, B., *Sensitivity analysis: from model parameters to system behaviour.* Essays in biochemistry, 2008. **45**: p. 177-194.
31. Zhang, X.Y., et al., *Sobol Sensitivity Analysis: A Tool to Guide the Development and Evaluation of Systems Pharmacology Models.* CPT Pharmacometrics Syst Pharmacol, 2015. **4**(2): p. 69-79.
32. Australian Building Codes Board, *National Construction Code Volume One*, in *Building Code of Australia*. 2019, Australian Building Codes Board: Canberra.
33. Cannavale, A., et al., *Building integration of semitransparent perovskite-based solar cells: Energy performance and visual comfort assessment.* Applied Energy, 2017. **194**: p. 94-107.
34. Cannavale, A., et al., *Improving energy and visual performance in offices using building integrated perovskite-based solar cells: A case study in Southern Italy.* Applied Energy, 2017. **205**: p. 834-846.
35. Dhaka, S., J. Mathur, and V. Garg, *Effect of building envelope on thermal environmental conditions of a naturally ventilated building block in tropical climate.* Building Services Engineering Research and Technology, 2013. **35**(3): p. 280-295.
36. Wang, Z. and J. Zhao, *Optimization of Passive Envelop Energy Efficient Measures for Office Buildings in Different Climate Regions of China Based on Modified Sensitivity Analysis.* Sustainability, 2018. **10**(4).
37. Bikas, D. and P. Chastas, *The Effect of the U Value in the Energy Performance of Residential Buildings in Greece.* Journal of Sustainable Architecture and Civil Engineering, 2014. **6**(1).
38. Rahmani, B., M.Z. Kandar, and P. Rahmani, *How double skin façade's air-gap sizes effect on lowering solar heat gain in tropical climate.* World Applied Sciences Journal, 2012. **18**(6): p. 774-778.
39. Peng, J., et al., *Numerical investigation of the energy saving potential of a semi-transparent photovoltaic double-skin facade in a cool-summer Mediterranean climate.* Applied Energy, 2016. **165**: p. 345-356.
40. Torres, M., et al., *Double skin facades - cavity and exterior openings dimensions for saving energy on Mediterranean climate.* Building Simulation, 2007. **26**(1): p. 198-205.
41. Parra, J., et al., *Thermal Performance of Ventilated Double Skin Façades with Venetian Blinds.* Energies, 2015. **8**(6): p. 4882-4898.
42. Lin, K. and S. Kato, *Field Experiments on Mechanical Double-skin System of Room-Side Air Gap in a Residential House.* Energy Procedia, 2015. **78**: p. 543-548.
43. Manikandan, S., *Measures of central tendency: Median and mode.* J Pharmacol Pharmacother, 2011. **2**(3): p. 214-5.
44. Mitalas, G.P. and J.G. Arseneault, *Fortran IV program to calculate z-transfer functions for the calculation of transient heat transfer through walls and roofs*. 1970: National Research Council Canada, Division of Building Research.
45. TRNSYS, *TRNSYS 17 - Volume 5 - Multizone building modelling with Type56 and TRNBuild*. 2005, Solar Energy Laboratory, University of Wisconsin-Madison: Madison, USA.

46. ASHRAE, *Standard 55-2017*, in *Thermal Environmental Conditions for Human Occupancy*. 2017, American Society of Heating, Refrigerating and Air Conditioning Engineers: Atlanta, Georgia.